

Ductility analysis of bolted extended end plate beam-to-column connections in the framework of the component method

Ana M. Girão Coelho[†]

*Department of Civil Engineering, Polytechnic Institute of Coimbra,
Rua Pedro Nunes, 3030-199 Coimbra, Portugal*

Luís Simões da Silva[‡]

*Department of Civil Engineering, University of Coimbra – Polo II,
Pinhal de Marrocos, 3030-290 Coimbra, Portugal*

Frans S. K. Bijlaard^{‡†}

*Steel and Timber Structures, Faculty of Civil Engineering and Geosciences,
Delft University of Technology, PO Box 5048, 2600 GA Delft, The Netherlands*

(Received January 4, 2005, Accepted July 25, 2005)

Abstract. The rotational behaviour of bolted extended end plate beam-to-column connections is evaluated in the context of the component method. The full moment-rotation response is characterized from the force-deformation curve of the individual joint components. The deformability of end plate connections is mostly governed by the bending of the column flange and/or end plate and tension elongation of the bolts. These components form the tension zone of the joint that can be modelled by means of “equivalent T-stubs”. A systematic analytical procedure for characterization of the monotonic force-deformation behaviour of individual T-stub connections is proposed. In the framework of the component method, the T-stub is then inserted in the joint spring model to generate the moment-rotation response of the joint. The procedures are validated with the results from an experimental investigation of eight statically loaded extended end plate bolted moment connections carried out at the Delft University of Technology. Because ductility is such an important property in terms of joint performance, particularly in the partial strength joint scenario, special attention is given to this issue.

Key words: analytical modelling; component method; deformation capacity; ductility; end plate connections; nonlinear materials; resistance; steel connections; stiffness; T-stub.

[†]Research Assistant, Corresponding author, E-mail: a.m.girao@clix.pt

[‡]Professor, E-mail: luisss@dec.uc.pt

^{‡†}Professor, E-mail: f.s.k.bijlaard@citg.tudelft.nl

1. Introduction

The analysis of steel-framed building structures with full strength beam-to-column joints is quite standard nowadays. Buildings utilizing such framing systems are widely used in design practice. However, there is growing recognition that there are significant benefits in designing joints as partial strength and semi-rigid (Steenhuis 1992). The design of joints within this partial strength/semi-rigid approach is becoming more and more popular. The use of such joints in steel frames, however, is only feasible if sufficient rotation capacity is developed so that a ductile failure mechanism of the whole structure can be formed prior to fracture of the joint. In general, end plate connections can achieve sufficient rotation capacity provided that the end plate or the column flange are “weak links” relative to the bolts. To meet the ductility requirements, the designer has to ensure that the required joint rotation, $\Phi_{j,req}$ is less than the available joint rotation, $\Phi_{j,avail}$:

$$\Phi_{j,req} \leq \Phi_{j,avail} \quad (1)$$

The behavioural characteristics of structural joints are commonly represented by means of a moment-rotation ($M-\Phi$) curve that defines three main properties: moment resistance, rotational stiffness and rotation capacity. Modern design codes, as the European code of practice for the design of structural steel joints in buildings, Eurocode 3 (CEN 2004), adopt the so-called component method for the prediction of this curve. For the purpose of simplicity, any joint can be subdivided into three different zones: tension, compression and shear. Within each zone, several sources of deformability can be identified, which are simple elemental parts (or “components”) that contribute to the overall response of the joint. Essentially, the method comprises three basic steps: (i) identification of the active components for a given structural joint, (ii) characterization of the individual component force-deformation ($F-\Delta$) response and (iii) assembly of those elements into a mechanical model made up of extensional springs and rigid links. This spring assembly is treated as a structure, whose $F-\Delta$ behaviour is used to generate the $M-\Phi$ curve of the full joint. From a theoretical point of view, this methodology can be applied to any joint configuration and loading conditions provided that the basic components are properly characterized.

In the case of thin end plate connections, the joint rotation mainly comes from the end plate deformation (Zandonini and Zanon 1988). For extremely thin end plates, the end plate deformation is sufficient to characterize the $M-\Phi$ curve since it is the only relevant joint component. In general, extended end plate connections are characterized by the participation of two or more components to the joint plastic deformation. In the framework of the component method, for this joint configuration, the following sources of deformability are identified (Fig. 1a): column web in shear (cws), column web in compression (cwc), column web in tension (cwt), column flange in bending (cfb), end plate in bending (epb), beam web and flange in compression (bfc), beam web in tension (bwt), bolts in tension (bt) and welds (w) (CEN 2004). Components column flange in bending, end plate in bending and bolts in tension are modelled as equivalent T-stubs. The full $M-\Phi$ response is derived from the $F-\Delta$ curve of the joint components, which are assembled into an appropriate mechanical model. Literature suggests alternative component models that share identical basic components but assume different component interplay (Weynand *et al.* 1995, Huber and Tschemmernegg 1998, Simões da Silva and Girão Coelho 2001, Borges 2003). Mechanical (component) models use a set of rigid and flexible parts (springs) to simulate the interaction between the various sources of joint deformation. The springs are combined in series or in parallel depending on the way they interplay with each other. Springs in series are subjected to the same force whilst parallel springs undergo the same deformation. The active components of a

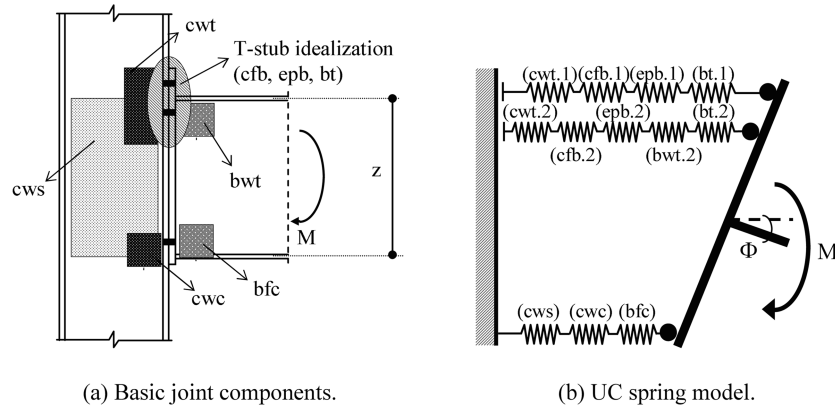


Fig. 1 Representation of an extended end plate connection with two bolt rows in tension (single-sided steel joint configuration)

joint are grouped according to their type of loading (tension, compression or shear). They can also be distinguished between those linked to the web panel, the load-introduction into the column web panel and the connection. Fig. 1(b) illustrates the mechanical model commonly used at the University of Coimbra (UC model hereafter) (Borges 2003, Girão Coelho 2004).

This paper focuses on the characterization of the rotational behaviour of bolted beam-to-column joints with an extended end plate and four bolts in tension, in the context of this component methodology. The full $M-\Phi$ curve is calculated by using a computational tool, NASCon (Borges 2003). This software allows for a multilinear definition of the deformation behaviour of the components and uses the spring model illustrated in Fig. 1(b). Because ductility is such an important property in a partial strength context, particular attention is given to this issue. The procedures are validated with experimental evidence. The eight experimental tests reported by the authors in Girão Coelho *et al.* (2004a) provide a comparison of moment resistance, rotational stiffness and ductility of similar joints with different end plate thickness and steel grade. The results illustrate the enhancement of ductility that is achieved by using thinner end plates and lower steel grades.

These experimental tests were basically aimed at the investigation of the end plate behaviour. The tension zone of the joint that is idealized within the T-stub approach was always critical. Therefore, the proposed methodology is illustrated and validated only for this connection type. However, from a theoretical point of view, the procedure can be applied to any beam-to-column joint configuration, as long as the $F-\Delta$ response of each component can be predicted with sufficient accuracy. This paper develops a simplified methodology for the evaluation of the nonlinear $F-\Delta$ response of those components modelled by equivalent T-stubs.

2. Modelling of bolt row behaviour through equivalent T-stubs

2.1. The T-stub idealization

The T-stub idealization of the tension zone of a connection consists in substituting this zone for T-stub sections of appropriate effective length, b_{eff} (Fig. 2). These T-stub sections are connected by their flange

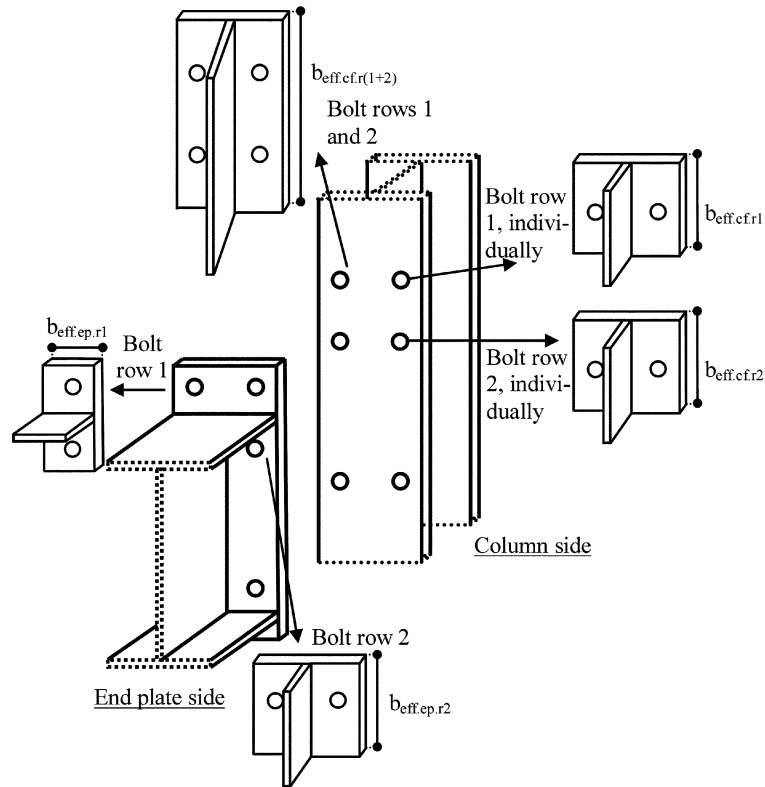
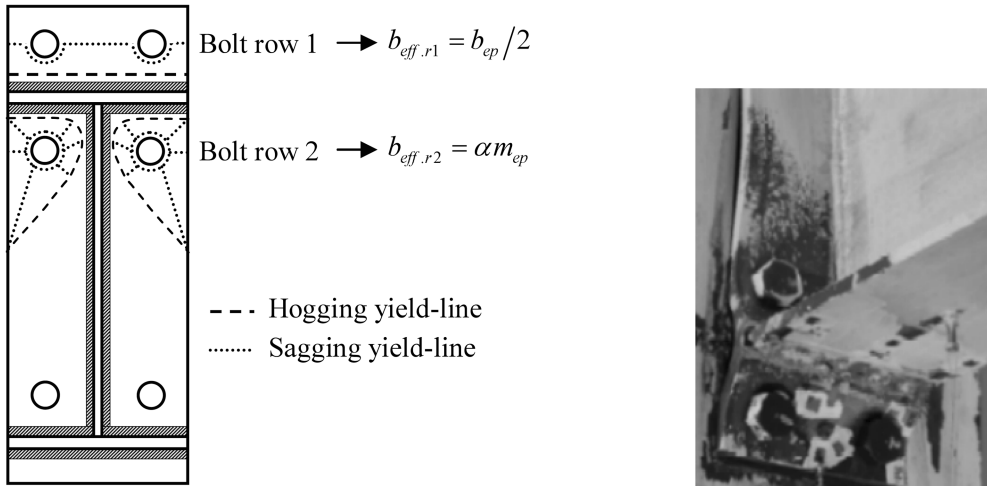


Fig. 2 T-stub idealization of an extended end plate bolted connection with two bolt rows in tension

to a rigid foundation (half-model) and subjected to a uniformly distributed force acting in the web plate (Adegoke and Kemp 2003). The extension of the end plate and the portion between the beam flanges are modelled as two separate equivalent T-stubs (index “ep”) (Fig. 2). On the column side (index “cf”), two situations have to be analysed: (i) the bolt rows act individually (index “r”) or (ii) the bolt rows act in combination (index “r(i+j)”) (Fig. 2).

The effective length of a T-stub is a notional width and does not necessarily represent any physical length of the flange. b_{eff} represents the width of the plate that contributes to load transmission and depends on the load level (elastic, yielding or near fracture). Hence, it must be established with respect to the desired property (initial elastic stiffness, plastic resistance or rotation capacity).

Zoetemeijer (1974) successfully introduced the T-stub concept in the context of the resistance of end plate connections. The effective length, in this case, accounts for all possible yield line mechanisms, either on the column side or the end plate side. It is defined by establishing the equivalence, in the plastic failure condition, between a beam model and the actual plate behaviour where collapse occurs due to the development of a yield line mechanism. Eurocode 3 presents expressions for evaluation of this parameter. In line with the upper bound method of plastic analysis, the value leading to the lowest plastic resistance has to be adopted, provided that it does not exceed the actual flange width. A typical observed yield-line pattern in thin end plates is shown in Fig. 3, for the case of an end plate with one bolt row below the tension beam flange. For thicker end plates, the patterns may not develop fully as the bolt elongation behaviour may govern the overall response. For end plates with more than one bolt



(a) Plot (after Adegoke and Kemp 2003)

(b) Illustration: FS1b (Girão Coelho *et al.* 2004a)

Fig. 3 Typical yield-line pattern in thin extended end plates with two bolt rows in tension

row below the flush line, the cases of individual and combined bolt row behaviour have to be taken into consideration.

2.2. Characterization of the individual T-stub behaviour

2.2.1. Introduction

The behaviour of an individual T-stub connection is typified in Fig. 4, which is usually described by the following properties: initial stiffness, $k_{e,0}$, post-limit stiffness, $k_{p-l,0}$, full plastic resistance, $F_{Rd,0}$, ultimate resistance, $F_{u,0}$ and deformation capacity, $\Delta_{u,0}$. In the paper these properties are evaluated per bolt row.

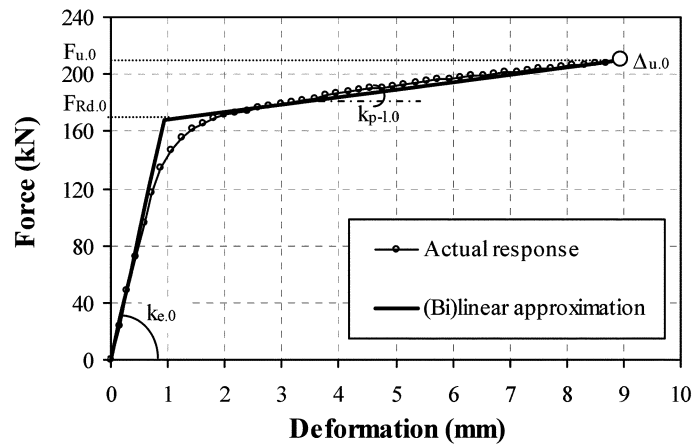


Fig. 4 Typical force-deformation response of an individual T-stub connection

Eurocode 3 provides design rules for the evaluation of $k_{e,0}$ and $F_{Rd,0}$, based on elastic theories (Yee and Melchers 1986, Jaspart 1991, 1997) and pure plastic theories (Zoetemeijer 1974, Packer and Morris 1977), respectively. The initial stiffness is evaluated as follows:

$$k_{e,0} = \frac{1}{2E \times 0.9 b_{eff} \left(\frac{t_f}{m}\right)^3 + 1.6E \frac{A_s}{L_b}} \quad (2)$$

where E is the Young modulus of steel, the length m represents the distance between the bolt axis and the section corresponding to the “potential” plastic hinge at the flange-to-web connection, A_s is the tensile stress area of a bolt and L_b is the conventional bolt length. According to Eurocode 3, $m = d - \zeta s$, where d represents the length between the bolt axis and the face of the T-stub element web, ζ is a coefficient taken as 0.8 and $s = r$ or $s = \sqrt{2}a_w$, for hot rolled profiles (HR-T-stubs) welded plates as T-stub (WP-T-stubs), respectively; r is the fillet radius of the flange-to-web connection and a_w is the throat thickness of the fillet weld.

The plastic resistance is taken as the smallest value among the three possible plastic failure modes (Fig. 5), i.e., $F_{Rd,0} = \min(F_{1,Rd,0}, F_{2,Rd,0}, F_{3,Rd,0})$, where:

$$F_{1,Rd,0} = \frac{4M_{f,Rd}}{m} \quad (3)$$

$$F_{2,Rd,0} = \frac{2M_{f,Rd} + 2B_{Rd}n}{m + n} \quad (4)$$

$$F_{3,Rd,0} = 2B_{Rd} \quad (5)$$

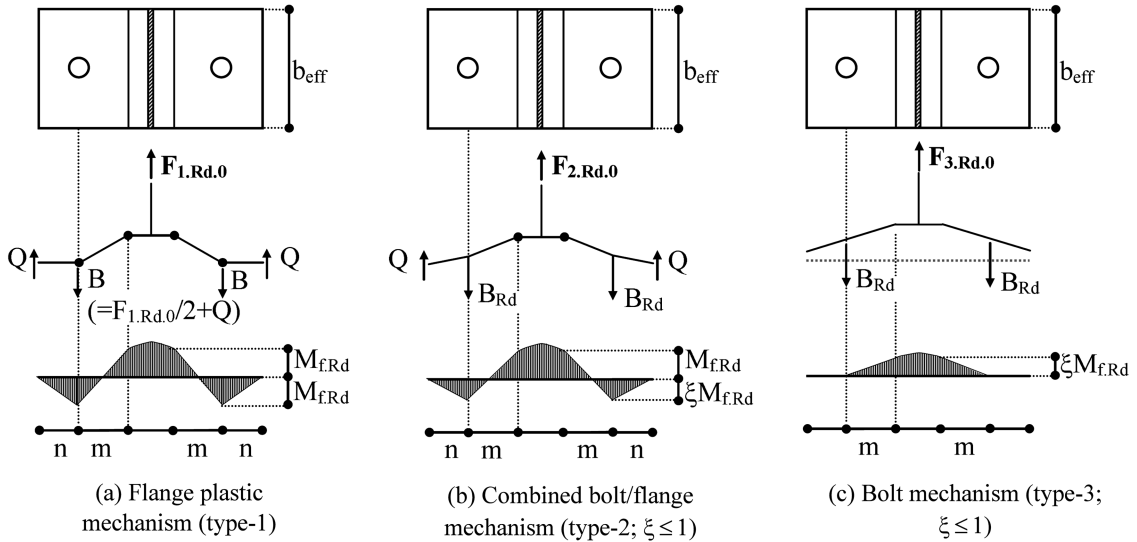


Fig. 5 Collapse mechanism typologies of a single T-stub connection at plastic conditions and distribution of internal actions

The plastic flexural resistance of the T-flanges, $M_{f,Rd}$, is given by:

$$M_{f,Rd} = \frac{t_f^2}{4} f_{yf} b_{eff} \quad (6)$$

where f_{yf} is the yield stress of the flanges and n is the effective edge distance. In Eurocode 3, n is taken as the minimum value of e (distance between the bolt axis and the tip of the flanges) and $1.25 m$, i.e., $n = \min(e, 1.25 m)$. B_{Rd} is the “plastic” (design) resistance of a single bolt in tension.

Eurocode 3 assumes elastic-perfectly plastic behaviour of the T-stub, with some implicit criteria to avoid brittle fracture. Consequently, the post-limit stiffness is taken as zero, which means that strain hardening and geometric nonlinear effects are neglected. Concerning the ductility, the code presents some qualitative principles based on the main contributions of the T-stub deformation: whenever the bending deformation of the flanges governs the plastic mechanism, the ductility is infinite; should the bolt determine collapse, the ductility is limited.

2.2.2. Previous research: nonlinear behaviour and ductility

Several theoretical approaches for the characterization of the overall nonlinear behaviour of individual T-stubs and its ductility have already been proposed in the literature (Jaspart 1991, Piluso *et al.* 2001, Swanson 1999). Essentially, they use the same basic prying mechanism, which is also the model implemented in Eurocode 3 (Fig. 6). The model is one-dimensional, i.e., the three-dimensional effects are not accounted for. The system is statically indeterminate to the first degree. It is loaded by applying a vertical force $F/2$ to the support (A), which is the critical section at the flange-to-web connection. F is the applied force per bolt row. Only one quarter-model is taken into account due to

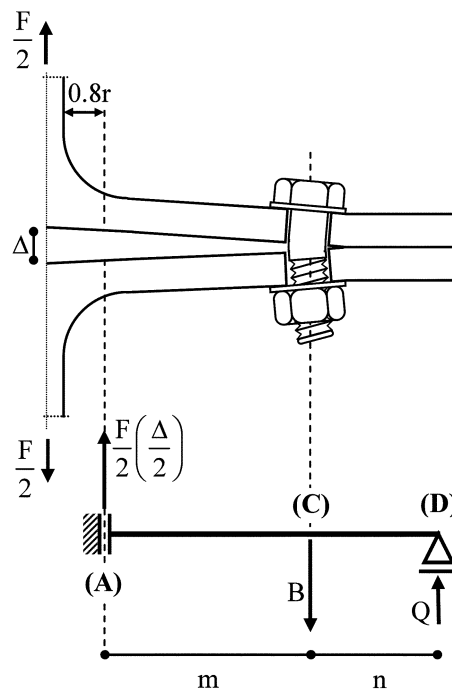


Fig. 6 T-stub basic prying mechanism

symmetry considerations. The contact points at the tip of the flange are modelled with a pinned support and reproduce the effect of the prying forces, Q . The T-stub flange behaves as a rectangular cross-section of width b_{eff} and (constant) depth equal to the flange thickness, t_f . Despite these major simplifications, the nonlinear analysis of this model is still complex and requires an incremental procedure. Thus, it is not intended for a hand computation unless some simplifications that reduce the model complexity to a reasonable level are assumed.

Jaspart approximates the nonlinear T-stub behaviour with a bilinear response (Jaspart 1991, 1997). The characteristics of this bilinear behaviour are summarized as follows:

- (i) The initial elastic region has a slope $k_{e,0}$ that is evaluated as in Eurocode 3 (Eq. (2)).
- (ii) The swivel point in the bilinear relationship represents the full development of the yield lines and the corresponding force is $F_{Rd,0}$. This plastic resistance is also computed according to the Eurocode 3 procedures (Eqs. (3-5)).
- (iii) In the plastic region, above the swivel point, the effects of material strain hardening are dominant. The slope of this second linear region is given by:

$$k_{p-l,0} = \frac{E_h}{E} k_{e,0} \quad (7)$$

where E_h is the strain hardening modulus.

(iv) The point of maximum force, $F_{u,0}$, is determined by formally equivalent expressions to $F_{Rd,0}$, by replacing the plastic conditions (index “Rd”) with ultimate conditions (index “u”). This means that these expressions are based on the same geometric characteristics but the plastic moment of the flange, $M_{f,Rd}$ is replaced with:

$$M_{f,u} = \frac{t_f^2}{4} f_{u,f} b_{eff} \quad (8)$$

where $f_{u,f}$ is the ultimate stress of the flange material and the bolt strength, B_u is given by:

$$B_u = \frac{B_{Rd}}{0.9} = f_{u,b} A_s \quad (9)$$

where $f_{u,b}$ is the ultimate stress of the bolt material. The deformation capacity is readily determined by intersection of the plastic region, with slope $k_{p-l,0}$, with the maximum resistance, $F_{u,0}$, i.e.,:

$$\Delta_{u,0} = \frac{F_{Rd,0}}{k_{e,0}} + \frac{(F_{u,0} - F_{Rd,0})}{k_{p-l,0}} \quad (10)$$

Piluso *et al.* (2001) developed an analytical procedure based on the resemblance of the distribution of internal forces at plastic and ultimate conditions. Fig. 5 shows the plastic conditions of a bolted T-stub for the three possible plastic failure modes and the corresponding internal forces. Their model disregards compatibility requirements between bolt and flange deformation. Cracking of the material is modelled by assuming the cracking condition as the occurrence of the ultimate strain in the extreme fibres of the T-stub flanges. The plastic deformation of the flange is computed from integration of the moment-curvature diagram, which is obtained from simple internal equilibrium conditions of the section and by assuming that the material constitutive law can be approximated by a quadrilinear relationship (in natural coordinates). This simple model yields a quadrilinear approximation of the $F-\Delta$

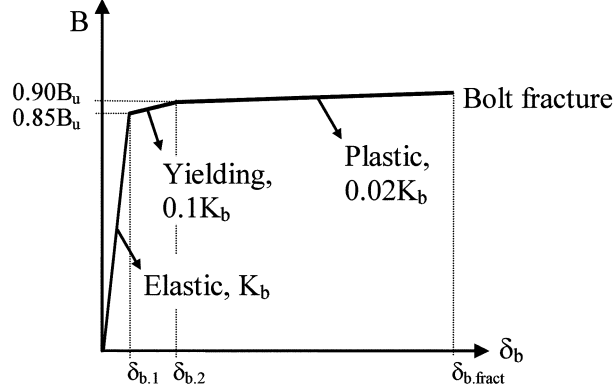


Fig. 7 Bolt force-deformation according to Swanson (1999)

curve. The ordinates of this curve are determined according to the potential failure mode (Fig. 5). In particular, for the evaluation of the force coordinates, they use formally equivalent expressions to the Eurocode 3 for plastic conditions.

Swanson (1999) developed a prying model that includes: (i) nonlinear material properties, (ii) a variable bolt stiffness that captures the changing behaviour of the bolts as a function of the loads they are subjected to, (iii) partial plastic hinges in the flange and (iv) second order membrane behaviour of thin flanges. The bolt behaviour is incorporated by means of an extensional spring located at the inside edge of the bolt shank. This spring is characterized by a piecewise linear force-deformation, B - δ_b , response (Fig. 7). The bolt elastic stiffness, K_b , is given by:

$$K_b = \frac{E_b}{\frac{L_s}{A_b} + \frac{L_{tg}}{A_s}} \quad (11)$$

where A_b is the nominal area of the bolt shank, L_s is the bolt shank length and L_{tg} is the bolt threaded length included in the grip. The bolt fracture deformation, $\delta_{b,fract}$, is computed as follows:

$$\delta_{b,fract} = 0.90 \frac{B_u L_s}{A_b E_b} + \varepsilon_{u,b} \left(L_{tg} + \frac{2}{n_{th}} \right) \quad (12)$$

where $\varepsilon_{u,b}$ denotes the ultimate bolt strain and n_{th} is the number of threads per unit length of the bolt. The flange mechanistic model assumes an elastic-yielding-plastic (with strain hardening) constitutive relationship for the steel. Plastic hinges develop at the flange-to-web connection and at the bolt axis. Swanson derived the stiffness coefficients and corresponding prying gradients by using the direct stiffness method. Both parameters are used in an incremental solution technique. First, the initial stiffness and prying gradient are determined. Next, several checks are made to determine which limit is reached first (bolt force or flange internal stresses limits). Incremental deformations are then calculated for each of the potential limits with the smallest value governing. The F - Δ curve can yield up to nine linear branches, with different stiffness, before failure. Swanson (1999) states

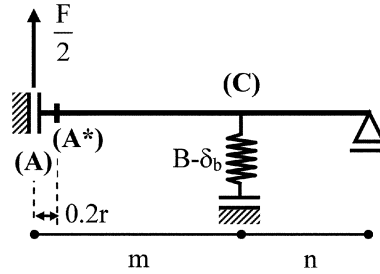


Fig. 8 Proposed T-stub model

that the strength and deformation capacity of the flange are not always predicted accurately because of sensitivities of the model to strain hardening parameters and bolt ductility. It should be stressed that the analysis of this model requires a computer routine.

2.2.3. Current proposal

The models described above afford some basis for the development of a model for evaluating the deformation capacity and the load-carrying capacity of T-stub connections as a standalone configuration. The model is depicted in Fig. 8, where the bolt behaviour is incorporated by means of an extensional spring located at section (C), i.e., at the bolt vertical axis. The bolt elongation response is reproduced with the tri-linear relationship proposed by Swanson (1999) (Fig. 7).

The flange material constitutive law is modelled by means of a piecewise (true) stress-(logarithmic) strain relationship that accounts for the strain hardening effects. From a design point of view, the nominal constitutive law is idealized by means of multilinear models that reproduce well the material strain hardening and fracture ranges, as depicted in Fig. 9 (Gioncu and Mazzolani 2002). Additionally, a reduction of the Young modulus of the flange material, E_{red} , is proposed (Girão Coelho 2004):

$$E_{red} = \frac{E}{3} \left(\frac{m}{t_f} \right)^2 \left[\sqrt{1 + \frac{3}{(m/t_f)^2}} - 1 \right] \quad (13)$$

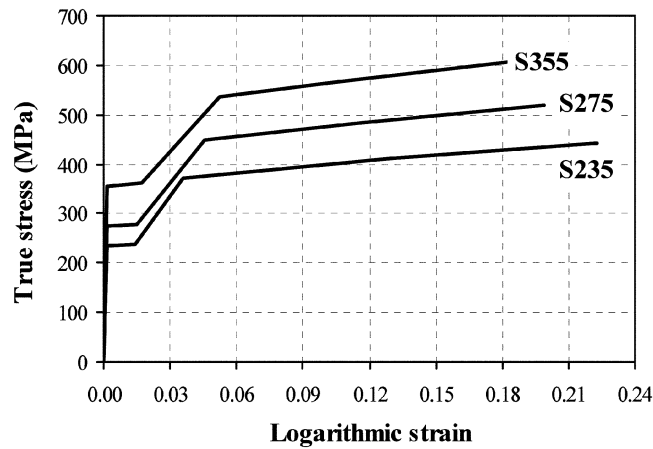


Fig. 9 Mechanical characteristics (true stress-logarithmic strain) for different nominal steel grades

Table 1 Geometrical and mechanical characteristics of the specimens (Fl: flange; Bt: bolt)

Test ID	Fracture element		Geometrical characteristics					Mechanical characteristics				
	Actual	Model pred.	b_{eff} (mm)	t_f (mm)	m (mm)	n (mm)	ϕ (mm)	$f_{y,f}$ (MPa)	$\varepsilon_{u,f}$	$f_{u,b}$ (MPa)	$\delta_{b,fract}$ (mm)	K_b (N/mm)
T1	Bt	Bt	40.0	10.7	29.45	30.00	12	431.0	0.284	974.0	0.97	6.92×10^5
P16	Bt	Bt	70.0	10.7	29.45	30.00	12	431.0	0.284	974.0	0.97	6.52×10^5
P18	Fl	Fl (A*)	70.0	10.7	29.45	30.00	20	431.0	0.284	974.0	1.09	1.73×10^6
WT1	Bt; fl	Fl (A*)	45.1	10.3	33.73	30.00	12	340.1	0.361	919.9	1.14	1.10×10^6
WT7_M16	Fl	Fl (A*)	74.9	10.3	33.89	29.80	16	340.1	0.361	919.9	2.60	1.65×10^6
WT7_M20	Fl	Fl (A*)	75.2	10.3	33.81	29.70	20	340.1	0.361	919.9	2.60	2.57×10^6
WT57_M12	Bt	Fl (A*)	75.0	10.1	34.11	30.20	12	698.6	0.174	919.9	4.00	9.14×10^5
WT57_M20	Bt; fl	Fl (A*)	75.1	10.2	34.27	30.20	20	698.6	0.174	919.9	2.60	2.57×10^6

Essentially, E_{red} incorporates a statistically calibrated factor that improves the analytical results when compared to the experiments. This reduction also accounts for the influence of the shear deformation of thick flanges in the elastic behaviour.

The two possible ultimate (fracture) conditions of the T-stub are: (i) fracture of the bolt and (ii) cracking of material of the flange near the web, i.e., at section (A*) (Fig. 8). This section (A*) is defined at a distance $m^* = d - r$ or $m^* = d - \sqrt{2}a_w$ for HR-T-stubs and WP-T-stubs, respectively.

The proposed methodology is illustrated below for some representative specimens from a database compiled by the authors (Girão Coelho 2004, Girão Coelho *et al.* 2004b) (see Table 1 and Fig. 10). The comparison with experimental or numerical (three-dimensional finite element model) evidence shows a good agreement of results in terms of stiffness and resistance (approximate errors: underestimation of ultimate resistance, $F_{u,0}$, in 15%, for those specimens whose cracking of the flange determines collapse and overestimation of circa 10% if collapse is governed by bolt fracture). In terms of ductility, the model predicts the deformation capacity accurately if the cracking of the flange is critical (see Figs. 10c, 10d, 10e). (For specimen WT1 (Fig. 10d), however, the bolt also fractured in the tests.) The exceptions in this case are the specimens made up of steel grade S690. Apparently, if the cracking condition is imposed as the attainment of the ultimate strain, ε_u , at section (A*), the deformation capacity, $\Delta_{u,0}$, is clearly underestimated (Fig. 10h). For those specimens whose plastic collapse involves a combined bolt/flange mechanism and eventually the bolt fractures (specimen P16, for instance - Fig. 10b), the prediction of $\Delta_{u,0}$ is good (average overestimation of 9% with a coefficient of variation of 11% for a sample of examples analysed in Girão Coelho 2004). At last, for those specimens exhibiting a flange plastic mechanism and fracture of the bolt at ultimate conditions, the agreement between actual and predicted values is not that satisfactory (predicted values nearly twice the actual values) (Fig. 10a).

The expression for the bolt elongation at fracture ($\delta_{b,fract}$), was derived for short-threaded bolts (Swanson 1999). If a full-threaded bolt is considered instead, this expression seems to overestimate the bolt fracture deformation. Therefore, in this case, the evaluation of $\delta_{b,fract}$ by application of the above expression should be cautious. Fig. 10(g) illustrates this setback with the bolt model applied to full-threaded bolts. In specimen WT57_M12 the flange plates are fastened by means of two full-threaded bolts. At collapse, the bolt model estimates a fracture elongation of 4 mm (Table 1). Since bolt governs fracture of this specimen, the post-limit behaviour proceeds until this deformation of 4 mm is attained, leading to an overall deformation of 8.1 mm and ultimate resistance of 174.5 kN, corresponding to 1.43 times the maximum resistance from the tests.

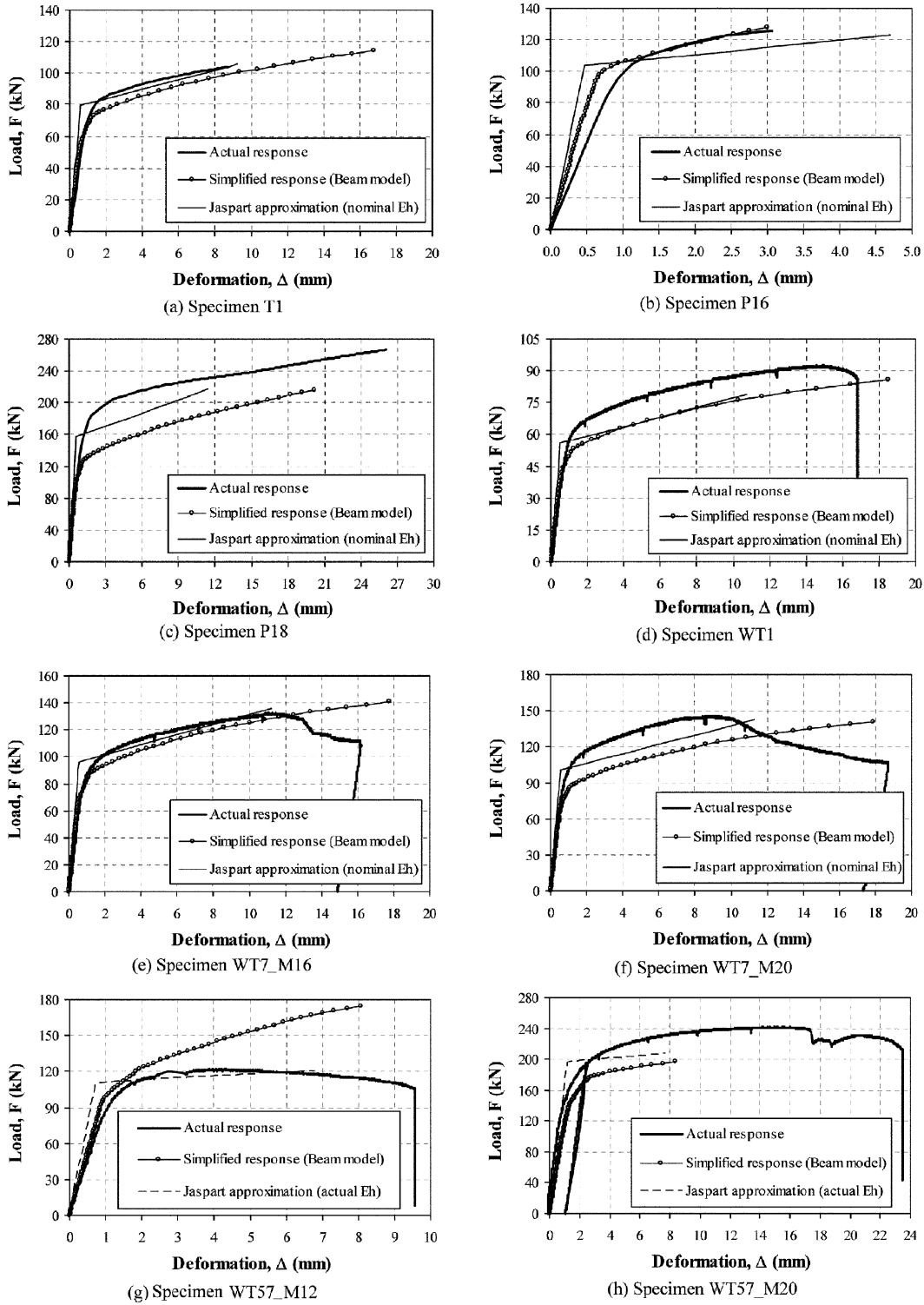


Fig. 10 Prediction of the force-deformation response of some T-stub specimens

In the above graphs, the bilinear predictions from Jaspert (1991) are also included. Generally speaking, the model reproduces well the actual behaviour for those specimens made up of S690 (Fig. 10g, for instance; for specimen WT57_M20, Fig. 10h, the predictions are particularly poor). For the remaining cases the predictions are fine provided that the nominal value of the strain hardening modulus ($E_{h,nom} = E/48.2$) is used. If the actual value of E_h is used instead, then the predictions are not as accurate (Girão Coelho 2004).

3. Application to bolted extended end plate connections

3.1. Description of the methodology

The methodology that is proposed for evaluation of the $M-\Phi$ response of bolted extended end plate joints, based on the component method, comprises the following steps:

(i) Characterization of the $F-\Delta$ curve of each joint component up to failure. In this particular case, all but the T-stub components remain elastic until failure. The T-stub components are modelled by multilinear representations for implementation in NASCon.

(ii) The overall $M-\Phi$ curve is generated using NASCon from the individual $F-\Delta$ component response.

(iii) The rotation capacity is determined when the first component reaches failure. In this specific case it is either the T-stub corresponding to the bolt row located at the end plate extension or that (those) corresponding to the other(s) bolt row(s) below the tension beam flange.

3.2. Comparison with experimental evidence

The four joint configurations selected for further comparisons, FS1-FS4, comprise two bolt rows in tension (Girão Coelho *et al.* 2004a). The geometrical characteristics of these specimens are set out in Table 2 and illustrated in Fig. 11. The specimens were designed to confine failure to the end plate and/or bolts without development of the full plastic moment capacity of the beam. The column behaves as a rigid element. Consequently, the tension zone on the end plate side that is idealized as a T-stub is always critical. For each test detail, on the end plate side, two equivalent T-stubs are identified (Fig. 2). For further reference, these two T-stubs are designated by “T-stub top” and “T-stub bottom”, for bolt rows 1 and 2, respectively (Fig. 2). The characterization of these components in terms of $F-\Delta$ behaviour is performed by means of three alternative procedures: (i) experimentally (available for the T-stub top of FS1, Fig. 10f, and FS4, Fig. 10h), (ii) analytically (proposed beam model) and (iii) simplified bilinear approximation proposed by Jaspert (1991).

Table 2 Details of the tested specimens

Test ID	#	Column		Beam		End plate	
		Profile	Steel grade	Profile	Steel grade	t_{ep} (mm)	Steel grade
FS1	2	HE340M	S355	IPE300	S235	10	S355
FS2	2	HE340M	S355	IPE300	S235	15	S355
FS3	2	HE340M	S355	IPE300	S235	20	S355
FS4	2	HE340M	S355	IPE300	S235	10	S690

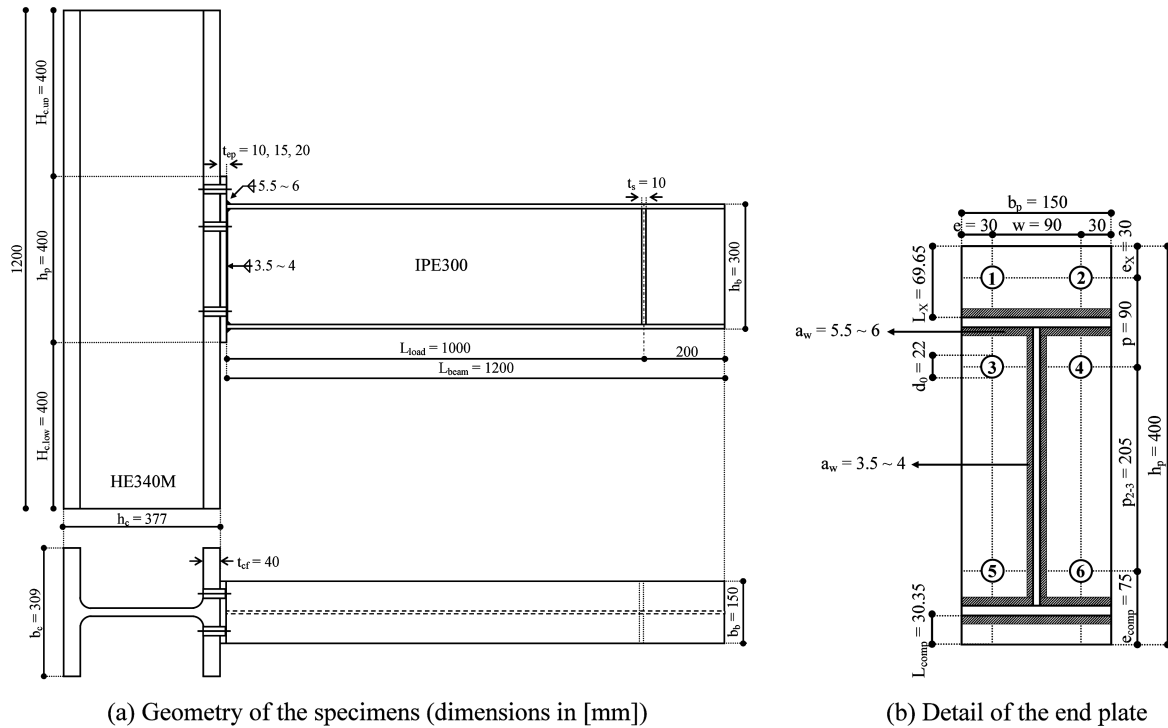


Fig. 11 Geometrical characteristics of the tested specimens

3.2.1. Component characterization

The effective length of the various T-stub components is defined according to Eurocode 3 and is summarized in Table 3. The actual geometric properties of the joints are used (Girão Coelho *et al.* 2004a). Fig. 12 illustrates the predicted $F-\Delta$ responses of some of the equivalent T-stubs. The remaining joint components behave elastically until collapse. The initial stiffness of these components was determined complying with the Eurocode 3 provisions.

For all T-stubs, the beam model predictions as well as the bilinear approximation proposed by Jaspart are assessed. The individual experimental results are not available for all equivalent T-stubs. For the equivalent T-stubs top from joints FS1 and FS4, the tests on WT7_M20 and WT57_M20, respectively, provide an experimental $F-\Delta$ curve that can be used for component characterization. The individual T-stub specimens do not correspond exactly to the equivalent T-stubs top as the bolt properties are different (Girão Coelho *et al.* 2004a, 2004b). Even though, no major differences are expected. The graphs also plot the experimental end plate deformation behaviour, which is obtained directly from the

Table 3 Effective length of the equivalent T-stubs

b_{eff} (mm)	Test ID			
	FS1	FS2	FS3	FS4
T-stub top	74.92	74.71	75.24	74.88
T-stub bot.	205.77	202.67	202.73	206.42

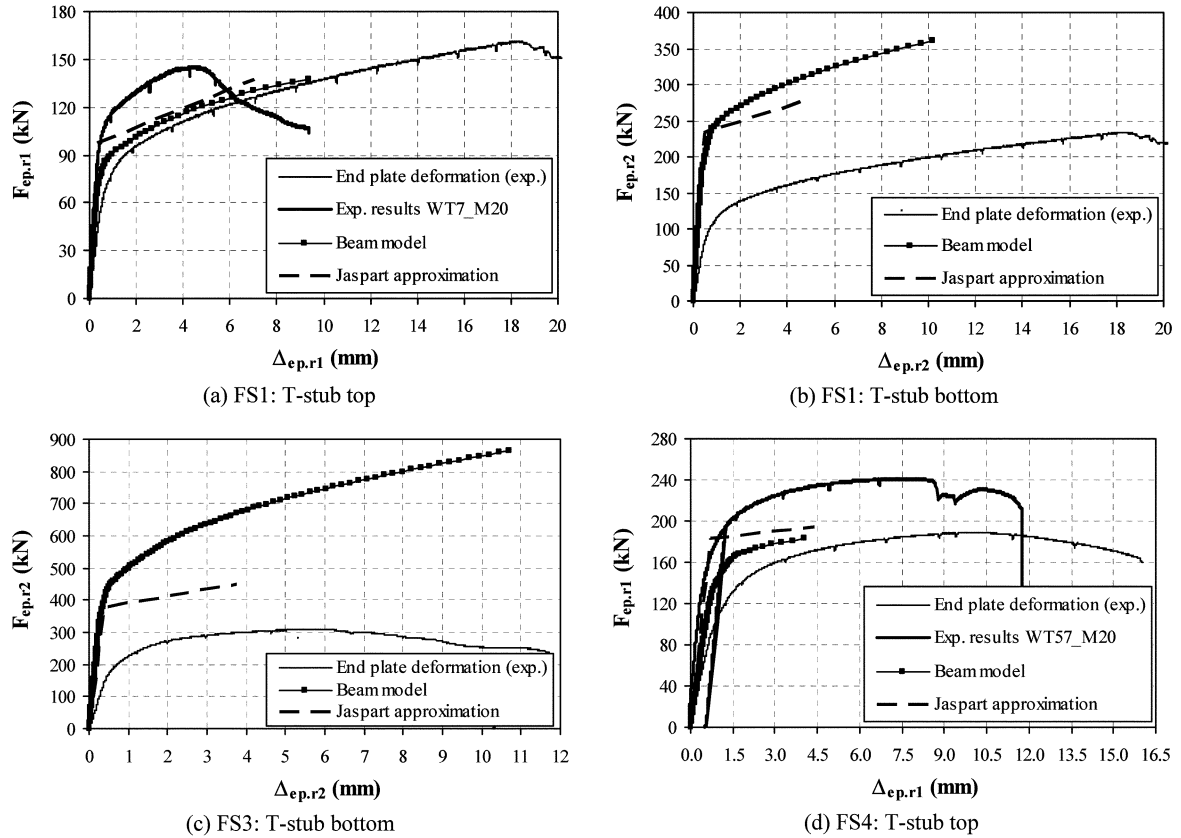


Fig. 12 Force-deformation behaviour for the equivalent T-stubs

measurement of the displacement of the tension beam flange with the course of loading. The corresponding force level is evaluated indirectly, $F_t = M/z$, whereby z is the lever arm. In these graphs, this force F_t acting at the level of the tension beam flange was divided equally by the two bolt rows. This procedure gives a good agreement with the predictions for T-stub top in FS1 (Fig. 12a) but deviates from the predicted behaviour for the T-stub bottom in the same case (Fig. 12b).

3.2.2. Evaluation of the nonlinear moment-rotation response

The full $M-\Phi$ joint response is evaluated using the software NASCon and using a displacement control-based strategy. The various curves are shown in the graphs from Fig. 13 and are compared with the experiments. The graphs trace the responses obtained with NASCon by introduction of the different characterization processes described above (BM: beam model; JA: Jaspart approximation; Exp: Experimental results for T-stub top and beam model for T-stub bottom). The critical component is also indicated in the graphs as well as the governing part (flange or bolt). Note that for different characterization processes, the determinant T-stub for rotation capacity can change (e.g. joint FS3 and the beam model or the bilinear approximation proposed by Jaspart for characterization of the T-stubs - Fig. 13c). The analysis of the curves shows that the analytical predictions: (i) overestimate the joint initial stiffness, $S_{j.mi}$ (e.g. specimen FS1 - $S_{j.mi.exp} = 17.5$ kNm/mrad, $S_{j.mi.BM} = 30.8$ kNm/mrad = 1.76 $S_{j.mi.Exp}$), (ii) the resistance can also be slightly overestimated by the rotation corresponding to

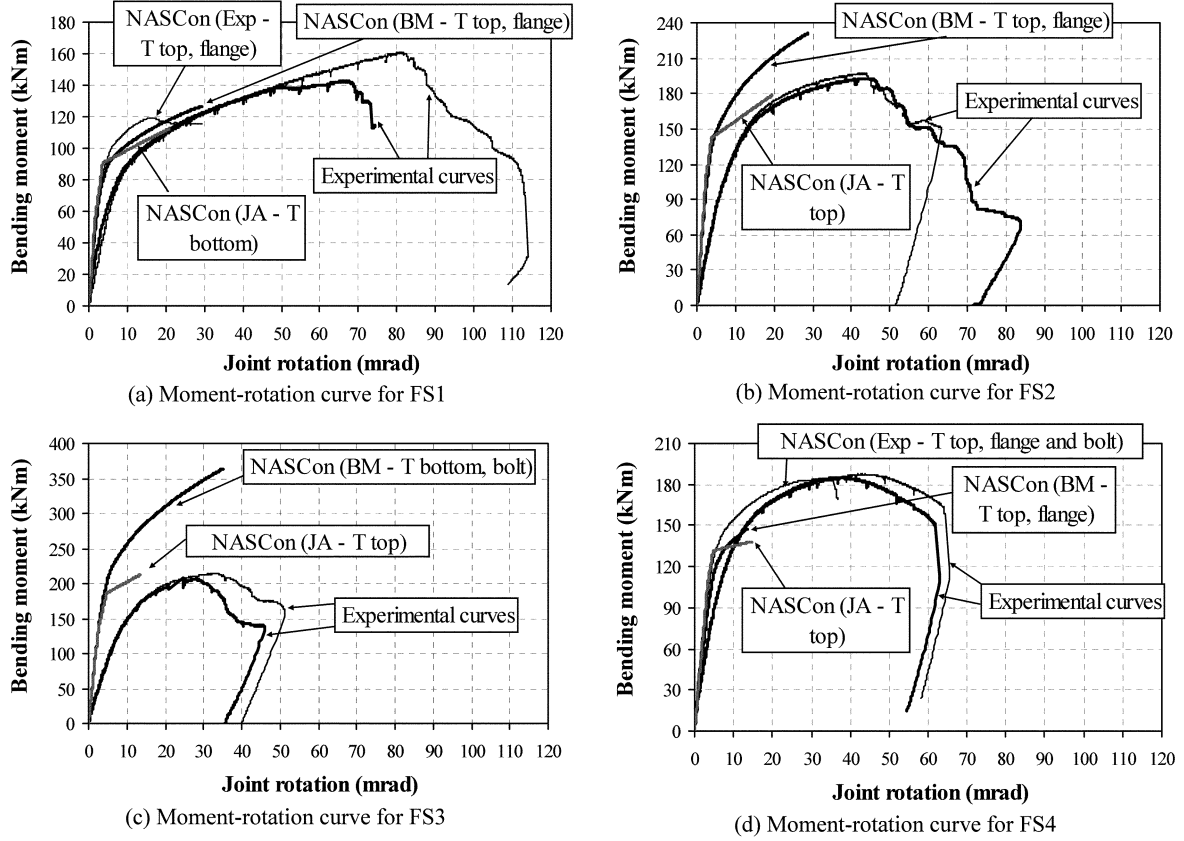


Fig. 13 Moment-rotation behaviour for the several joints

maximum load level ($\Phi_{M_{max}}$) analytical predictions, particularly in the plastic domain (e.g. FS3, Fig. 13c) though for thinner end plates the predictions are good (e.g. FS1, FS4, Figs. 13a,d) and (iii) the rotation capacity (Φ_{Cd}) is clearly underestimated by the analytical methods, even for the cases of FS1 and FS4 with the experimental component characterization. Table 4 sets out the rotation predictions (experimental and analytical). Experimentally, three rotation values are evaluated: the rotation at which the moment first reaches $M_{j,Rd}$, Φ_{Xd} , $\Phi_{M_{max}}$ and the rotation capacity, Φ_{Cd} . $M_{j,Rd}$ is the joint (experimental) plastic resistance, as defined by Jaspert (1991). Analytically, the rotation capacity is attained when the first component reaches failure. The experimental values in Table 3 are the averaged values between the tests for each configuration, except for FS1 and FS3 for which the value of tests “b” are adopted (Girão Coelho *et al.* 2004a).

3.2.3. Characterization of the joint ductility

The ductility of a joint can be defined as the amount of plastic rotation that can be sustained while maintaining a certain percentage of its ultimate strength (Swanson 1999). It reflects the length of the yield plateau of the M - Φ response. This property can be quantified by means of an index Ψ_j that relates the rotation capacity of the joint, Φ_{Cd} to the rotation value corresponding to the joint plastic resistance, Φ_{Xd} (Simões da Silva *et al.* 2002):

Table 4 Comparison of the predictions of rotation of the various joints (in [mrad])

Test ID	Experimental predictions			Analytical predictions					
				BM		JA		Exp	
	Φ_{Xd}	$\Phi_{M_{max}}$	Φ_{Cd}	Φ_{Xd}	Φ_{Cd}	Φ_{Xd}	Φ_{Cd}	Φ_{Xd}	Φ_{Cd}
FS1	6.5	77.1	111.2	3.0	29.2	2.4	21.0	3.3	29.5
FS2	7.4	41.0	71.9	3.4	28.8	3.0	19.4	-	-
FS3	8.9	30.0	48.7	4.4	35.0	3.4	13.5	-	-
FS4	9.9	40.8	63.0	5.0	13.5	4.0	14.6	4.4	36.8

Table 5 Evaluation of the joint ductility index Ψ_j for the various configurations

Test ID	Experimental predictions		Analytical predictions					
			BM		JA		Exp	
	$(\Phi_{M_{max}} / \Phi_{Xd})$	(Φ_{Cd} / Φ_{Xd})	$\Phi_{Xd, anl}$	$\Phi_{Xd, exp}$	$\Phi_{Xd, anl}$	$\Phi_{Xd, exp}$	$\Phi_{Xd, anl}$	$\Phi_{Xd, exp}$
FS1	11.86	17.11	9.73	4.49	8.75	3.23	8.94	4.54
FS2	5.54	9.72	8.47	3.89	6.47	2.62	-	-
FS3	3.37	5.47	7.95	3.93	3.97	1.52	-	-
FS4	4.12	6.36	2.70	1.36	3.65	1.47	8.36	3.72

$$\Psi_j = \frac{\Phi_{Cd}}{\Phi_{Xd}} \quad (14)$$

Table 5 evaluates the joint ductility index for the various joints (cf. rotation values in Table 4). The table contains the experimental evaluation of the ductility index for $\Phi_{M_{max}}$ (second column) and the rotation capacity, Φ_{Cd} (third column). The difference between the two indexes varies from 30% for FS1 and 43% for FS2. For the analytical procedures, the ductility index was evaluated at the analytical value for rotation capacity but with respect to the analytical (index “anl”) and experimental (index “exp”) values of F_{Xd} , as shown in Table 5. For the BM analytical predictions, the differences are not relevant. For the other two processes the index Ψ_j evaluated with respect to $\Phi_{Xd, exp}$ is bigger.

The analytical predictions of the ductility index are quite severe, particularly for the thinner end plate specimens, FS1 and FS4 (3rd-4th columns, Table 5). This situation also results from the underestimation of the T-stub component ductility itself (e.g. FS4, Fig. 12d). The analytical predictions for deformation capacity of the individual T-stubs are rather conservative, as seen above. Consequently, the rotation capacity of the overall joint, which is calculated from the individual components contribution, is also underestimated. On the contrary, for specimen FS3 that uses a 20 mm thick end plate, the ductility index is overestimated (3rd-4th columns, Table 5).

4. Conclusions

The rotational behaviour of bolted extended end plate beam-to-column connections was evaluated in the context of the component method. The methodology was restricted to joints whose behaviour was governed by the end plate modelled as equivalent T-stubs in tension. It has been shown that the overall $M-\Phi$ characteristics can be modelled fairly accurately provided that the T-stub component $F-\Delta$ behaviour is well characterized. The analytical models for the individual T-stubs and for the assessment

Table 6 Verification of the recommendations for rotation capacity

Test ID	t_{ep} (mm)	Maximum t_{ep} (mm)	Verification of Eq. (15)
FS1	10.40	11.80	Yes.
FS2	15.01	11.75	No.
FS3	20.02	11.76	No.
FS4	10.06	8.25	<i>No.</i>

of the joint rotational response have shown a good agreement with the experimental results.

Because ductility is such an important characteristic in connection performance, the evaluation of the joint rotation capacity, i.e., the available joint rotation, was addressed with greater depth. Eurocode 3 (CEN 2004) states that a bolted end plate joint may be assumed to have sufficient rotation capacity for plastic analysis, provided that both of the following conditions are satisfied: (i) the moment resistance of the joint is governed by the resistance of either the column flange in bending or the end plate in bending and (ii) the thickness t of either the column flange or the end plate (not necessarily the same basic component as in (i)) satisfies:

$$t \leq 0.36 \phi \sqrt{\frac{f_{u,b}}{f_y}} \quad (15)$$

where ϕ is the bolt diameter, $f_{u,b}$ is the tensile strength of the bolt and f_y is the yield stress of the relevant basic component. Application of these guidelines to the characterization of the rotation capacity shows that the first condition is guaranteed for all specimens (the joint moment resistance is always governed by the resistance of the end plate in bending), whilst the second condition, Eq. (15), is only fulfilled for specimens FS1 (Table 6). Though these recommendations are only valid for steel grades up to S460, they were also applied to series FS4 that includes end plates from grade S690 (value in *italic*).

It is generally accepted that a minimum of 40-50 mrad ensures “sufficient rotation capacity” of a bolted joint in a partial strength scenario. Table 4 shows that joints FS2 and FS4 also guarantee this condition at maximum load. Therefore, the Eurocode 3 current provisions seem too conservative as far as rotational capacity is concerned. This study affords some basis for the proposal of some additional criteria on this topic. From the analysis of the ductility indexes in Table 5, computed at maximum load, a minimum joint ductility index of 4.0 seems appropriate in order to ensure “sufficient rotation capacity”. This limitation should be set in conjunction with an absolute minimum value of 40 mrad and is valid for steel grade S355. For steel grade S690 similar criteria might be established. However, the T-stub component as a standalone configuration has to be further explored for higher steel grades because of the inherent specificities. In addition, the analytical procedure has to be calibrated with other joint specimens since the joint ductility indexes are not yet accurate enough (cf. Table 5).

Naturally, as the above mentioned joints were designed to confine failure to the end plate and bolts, the deformation behaviour is exclusively dependent on these two components that form an equivalent T-stub. Therefore, the conclusions are only valid if the T-stub on the end plate side determines collapse.

Finally, although it has been shown that deemed-to-satisfy criteria for sufficient rotation capacity stated in Eurocode 3 are overconservative, the establishment of more accurate criteria still requires further work.

Acknowledgments

Financial support from the Portuguese Ministry of Science and Higher Education (*Ministério da Ciência e Ensino Superior*) under contract grants from PRODEP and FCT (Grant SFRH/BD/5125/2001) for Ana M. Girão Coelho is gratefully acknowledged. This research was supported in part by the FCT research project POCI/ECM/55783/2004.

References

- Adegoke, I.O. and Kemp, A.R. (2003), "Moment-rotation relationships of thin end plate connections in steel beams", *Proc. of the Int. Conf. on Advances in Structures, ASSCCA'03* (Eds.: G.J. Hancock, M.A. Bradford, T.J. Wilkinson, B. Uy and K.J.R. Rasmussen), Sydney, Australia, 119-124.
- Borges, L.A.C. (2003), "Probabilistic evaluation of the rotation capacity of steel joints", MSc Thesis, University of Coimbra, Coimbra, Portugal.
- European Committee for Standardization (CEN). (2004), *PrEN 1993-1-8:2004, Eurocode 3: Design of steel structures, Part 1.8: Design of joints*, Stage 49, June 2004, Brussels.
- Gioncu, V. and Mazzolani, F.M. (2002), *Ductility of Seismic Resistant Steel Structures*. Spon Press, London, UK.
- Girão Coelho, A.M. (2004), "Characterization of the ductility of bolted end plate beam-to-column steel connections", PhD Thesis, University of Coimbra, Coimbra, Portugal.
- Girão Coelho, A.M., Bijlaard, F. and Simões da Silva, L. (2004a), "Experimental assessment of the ductility of extended end plate connections". *Engrg. Struct.*, **26**, 1185-1206.
- Girão Coelho, A.M., Bijlaard, F., Gresnigt, N. and Simões da Silva, L. (2004b), "Experimental assessment of the behaviour of bolted T-stub connections made up of welded plates". *J. Const. Steel Res.*, **60**, 269-311.
- Huber, G. and Tschemmernegg, F. (1998), "Modelling of beam-to-column joints". *J. Const. Steel Res.*, **45**, 199-216.
- Jaspart, J.P. (1991), "Study of the semi-rigid behaviour of beam-to-column joints and of its influence on the stability and strength of steel building frames", PhD Thesis (in French), University of Liège, Liège, Belgium.
- Jaspart, J.P. (1997), "Contributions to recent advances in the field of steel joints - column bases and further configurations for beam-to-column joints and beam splices", Aggregation Thesis, University of Liège, Liège.
- Packer, J.A. and Morris, L.J. (1977), "A limit state design method for the tension region of bolted beam-to-column connections". *The Structural Engineer*, **55**(10), 446-458.
- Piluso, V., Faella, C. and Rizzano, G. (2001), "Ultimate behaviour of bolted T-stubs. I: theoretical model". *J. Struct. Engrg. ASCE*, **127**(6), 686-693.
- Simões da Silva, L.A.P. and Girão Coelho, A.M. (2001), "A ductility model for steel connections". *J. Const. Steel Res.*, **57**, 45-70.
- Simões da Silva, L., Santiago, A. and Vila Real, P. (2002), "Post-limit stiffness and ductility of end plate beam-to-column steel joints". *Comp. & Struct.*, **80**, 515-531.
- Steenhuis, C.M. (1992), "Frame design and economy", *Proc. of the state-of-the-art workshop Semi-rigid behaviour of Civil Engineering structural connections* (Ed.: A. Colson), Strasbourg, France, 549-559.
- Swanson, J.A. (1999), "Characterization of the strength, stiffness and ductility behaviour of T-stub connections", PhD Thesis, Georgia Institute of Technology, Atlanta, USA.
- Weynand, K., Jaspart, J.P. and Steenhuis, M. (1995), "The stiffness model of revised annex J of Eurocode 3". *Proc. of the 3rd Int. Workshop on connections, Connections in Steel Structures, Behaviour, strength and design* (Eds.: R. Bjorhovde, A. Colson, R. Zandonini) Trento, Italy, 441-452.
- Yee, Y.L. and Melchers, R.E. (1986), "Moment-rotation curves for bolted connections". *J. Struct. Engrg. ASCE*, **112**(3), 615-635.
- Zandonini, R. and Zanon, P. (1988), "Experimental analysis of end plate connections". *Proc. of the 1st Int. Workshop on connections, Connections in Steel Structures, Behaviour, strength and design* (Eds.: R. Bjorhovde, J. Brozzetti, A. Colson), Cachan, France, 40-51.
- Zoetemeijer, P. (1974), "A design method for the tension side of statically loaded bolted beam-to-column connections", *Heron*, **20**(1), 1-59.

Notation

Lower cases

a_w	: Throat thickness of a fillet weld
b	: Width
b_{eff}	: Effective width of a T-stub tributary to a bolt row for resistance calculations
d	: Length between the bolt axis and the face of the T-stub web
d_0	: Bolt hole clearance
e	: Edge distance
f_u	: Ultimate or tensile stress
f_y	: Yield stress
h	: Height
$k_{e,0}$: Initial stiffness of an individual T-stub connection
$k_{p-l,0}$: Post-limit stiffness of an individual T-stub connection
m	: Distance from bolt centre to 20% distance into profile root or weld
m^*	: Distance from bolt centre to profile root or weld
n	: Effective edge distance
n_{th}	: Number of threads per unit length of the bolt
p	: Pitch of the bolts
r	: Fillet radius of the flange-to-web connection
s	: Length
t	: Thickness
w	: Gauge of the bolts
z	: Lever arm; Cartesian axis

Upper cases

A_b	: Nominal area of the bolt shank
A_s	: Bolt tensile stress area
B	: Bolt force
E	: Young modulus
E_h	: Strain hardening modulus
F	: Force; resistance; load; applied force per bolt row in the case of an individual T-stub connection
$F_{Rd,0}$: Full “plastic” (design) resistance of an individual T-stub connection
F_t	: Force acting at the level of the tension beam flange statically equivalent to the applied bending moment M
$F_{u,0}$: Ultimate resistance of an individual T-stub connection
H	: Height
K_b	: Bolt elastic stiffness according to the Swanson’s bolt model
L	: Length
L_b	: Bolt conventional length
L_s	: Bolt shank length
L_{tg}	: Bolt threaded length included in the grip length
M	: Bending moment
M_f	: Flexural resistance of the T-stub flanges
$M_{j,Rd}$: Joint flexural plastic (design) resistance
Q	: Prying force
$S_{j,ini}$: Initial rotational stiffness of a joint

Greek letters

α	: Coefficient obtained from an abacus provided in Eurocode 3
δ_b	: Elongation of a bolt

Δ	: Axial deformation
$\Delta_{u,0}$: Deformation capacity of an individual T-stub connection
ε	: Strain; engineering strain; parameter
ε_u	: Ultimate strain
ϕ	: Bolt diameter
Φ	: Joint rotation
Φ_{Cd}	: Rotation capacity of a joint
$\Phi_{j,avail}$: Available joint rotation
$\Phi_{j,req}$: Required joint rotation
$\Phi_{M_{max}}$: Rotation of the joint at maximum load
Φ_{Xd}	: Joint rotation value at which the moment resistance first reaches $M_{j,Rd}$
ξ	: Coefficient
Ψ_j	: Joint ductility index
ζ	: Coefficient taken as 0.8 in Eurocode 3

Subscripts

anl	: Analytical result
<i>b</i>	: Bolt
<i>cf</i>	: Column flange
<i>ep</i>	: End plate
exp	: Experimental result
<i>f</i>	: Flange
<i>fract</i>	: Fracture
<i>j</i>	: Joint
nom	: Nominal property
<i>ri</i>	: Bolt row <i>i</i>
<i>r(i+j)</i>	: Bolt rows <i>i</i> and <i>j</i>
<i>red</i>	: Reduced
<i>Rd</i>	: Pure plastic conditions; design conditions
<i>u</i>	: Ultimate
<i>w</i>	: Weld
<i>X</i>	: End plate extension
<i>y</i>	: Yield

CC